Article

Prev. | Next | Table of Contents

Hydrophilic Dots on Hydrophobic Nanopatterned Surfaces as a Flexible Gas Barrier

Jin Hwan Choi, Young Min Kim, Young Wook Park, Tae Hyun Park, Ki Young Dong and Byeong Kwon Ju*
Display and Nanosystem Laboratory, College of Engineering, Korea University, 5-1 Anam-Dong, Seongbuk-Gu, Seoul 136-701, Korea

Abstract | Supporting Info | Full Text HTML | Figures | Hi-Res PDF [3088 KB] | References | PDF w/ Links [864 KB]

Langmuir, 2009, *25* (12), pp 7156-7160
DOI: 10.1021/la804325x
Publication Date (Web): May 11, 2009

*Author to whom correspondence should be addressed [e-mail bkju@korea.ac.kr; telephone +82-(0)2-3290-3671; fax +82-(0)2-3290-3791].

Article Tools
Add to Favorites
Download Citation
Email a Colleague
Permalink
Order Reprints
Rights & Permissions
Citation Alerts

SciFinder Links
SciFinder®
View Reference Detail

Related Content
Other ACS articles by these authors:
Jin Hwan Choi
Young Min Kim
Young Wook Park
Tae Hyun Park
Ki Young Dong
Byeong Kwon Ju

Abstract

Langmuir
Article
pubs.acs.org/Langmuir

Hydrophilic Dots on Hydrophobic Nanopatterned Surfaces as a Flexible Gas Barrier

Jin Hwan Choi, Young Min Kim, Young Wook Park, Tae Hyun Park, Ki Young Dong, and Byeong Kwon Ju*

Display and Nanosystem Laboratory, College of Engineering, Korea University, 5-1 Anam-Dong, Seongbuk-Gu, Seoul 136-701, Korea

Received December 31, 2008. Revised Manuscript Received February 11, 2009

The present study demonstrates a transparent polymeric gas barrier film mimicking the Namib Desert beetle's back. SiO_2 hydrophilic dots have been deposited on a nanopatterned hydrophobic surface. A nanopatterned surface was fabricated by UV-curable nanoimprinting techniques. The surface energies of the hydrophobic and hydrophilic domains were 7.29 and > 73.12 mN/m, respectively. The characteristics of water vapor transfer from hydrophobic to hydrophilic regions due to difference of the attractive force at interfaces are shown to yield the enhanced barrier performance according to the Ca degradation measurements. This strategy is suitable for organic electronics, solar cells, and plastic optics applications requiring moisture-free properties with high transmission.

Introduction

As the next-generation technology, the use of plastic substrates enables the fabrication of new applications in the area of flexible displays, solar cells, and opto-devices. Despite the many advantages that the plastics potentially offer the industrial sector, polymer substrates possess material limitations. Plastic film presents major challenges such as high flexibility, thermal stability, optical transparency, and especially moisture barrier efficiency. A major limitation of plastic film is moisture permeation through the substrates and moisture-induced degradation of polymeric materials. Due to the extreme requirements for barrier efficiency, increasing efforts have been made to gain a better understanding of the moisture permeation mechanism with an intent to enhance barrier efficiency using various kinds of silica- and alumina-based materials.[1,2]

Besides the bulk protective coating technologies, controlling moisture movement at the barrier surfaces is an effective technology for low moisture permeation rates. A means for controlling the wetting behavior can be offered by patterned surfaces in nature.[3−5] The Stenocara beetle in the Namib Desert uses a hydrophilic/hydrophobic patterned surface on its back to collect drinking water from fog-laden wind.[6−8] Parker and co-workers[6] found that the structure of the beetle's back enabled this unique water-collecting ability; a random array of smooth hydrophilic bumps is present on the Stenocara beetle's back (0.5 mm in size and arranged 0.5−1.5 mm apart). These hydrophilic regions are surrounded by hydrophobic areas comprising physical features (approximately 10 μm in size), arranged in a hexagonal array, reminiscent of the lotus leaf.[6,9,10]

This moisture-controlling property is important for various technological applications including biomolecules,[11] microfluidics,[12] and the formation of moisture-free protective layers[2] from both fundamental and practical aspects. Also, these structures have inspired scientists to generate superhydrophobic surfaces using a variety of methods such as plasma treatments,[8,13] UV−ozone exposure,[4] sublimation,[14] and chemical vapor deposition.[15] However, some of these approaches often suffer from the drawback of being a short-lived effect or causing thermionic damage to low T_g polymeric substrates. Also, long-term durability is an important property for the protection of organic materials that have poor chemical, thermal, or mechanical stabilities. As the hydrophobicity is influenced by both the surface energy of the coating materials and the surface roughness, the surface structures are also important in enhancing the hydrophobicity. For this reason, the various fractal micro- and nanostructures, for example, nanotubes,[15] nanofilaments,[16] nanopins,[17] and nanorods,[18] have been introduced as superhydrophobic surface structures.

In these applications, we have fabricated transparent gas barrier surfaces by mimicking the Stenocara beetle's back. SiO_2 hydrophilic dots have been deposited on a nanopatterned hydrophobic polymer surface. A highly transparent and nanostructured hydrophobic surface has been fabricated by imprinting technique.[19] The patterned area should have a consistent, uniform

*Author to whom correspondence should be addressed [e-mail bkju@korea.ac.kr; telephone + 82-(0)2-3290-3671; fax + 82-(0)2-3290-3791].

(1) Chwang, A. B.; Rothman, M. A.; Mao, S. Y.; Hewitt, R. H.; Weaver, M. S.; Silvernail, J. A.; Rajan, K.; Hack, M.; Brown, J. J.; Chu, X.; Moro, L.; Krajewski, T.; Rutherford, N. *Appl. Phys. Lett.* **2003**, *83*, 413.
(2) Carcia, P. F.; Mclean, R. S.; Reilly, M. H.; Groner, M. D.; George, S. M. *Appl. Phys. Lett.* **2006**, *89*, 031915.
(3) Zhang, F.; Low, H. Y. *Langmuir* **2007**, *23*, 7793.
(4) Han, J. T.; Kim, S.; Karim, A. *Langmuir* **2007**, *23*, 2608.
(5) Lenz, P. *Adv. Mater.* **1999**, *11*, 1531.
(6) Parker, A. R.; Lawrence, C. R. *Nature (London)* **2001**, *414*, 33.
(7) Zhai, L.; Berg, M. C.; Cebeci, F. C.; Kim, Y.; Milwid, J. M.; Rubner, M. F.; Cohen, R. E. *Nano Lett.* **2006**, *6*, 1213.
(8) Garrod, R. P.; Harris, L. G.; Schofield, W. C. E.; Mcgettrick, J.; Ward, L. J.; Teare, D. O. H.; Badyal, J. P. S. *Langmuir* **2007**, *23*, 689.
(9) Zhang, X.; Shi, F.; Niu, J.; Jiang, Y.; Wang, Z. *J. Mater. Chem.* **2008**, *18*, 621.
(10) Lee, S. M.; Kwon, T. H. *J. Micromech. Microeng.* **2007**, *17*, 687.
(11) Macbeath, G.; Schreiber, S. L. *Science* **2000**, *289*, 1760.
(12) Lam, P.; Wynne, K. J.; Wnek, G. E. *Langmuir* **2002**, *18*, 948.
(13) Kim, C. S.; Jo, S. J.; Kim, J. B.; Ryu, S. Y.; Noh, J. H.; Biak, H. K.; Lee, S. J.; Kim, Y. S. *Appl. Phys. Lett.* **2007**, *91*, 063503.
(14) Nakajima, A.; Fujishima, A.; Hashimoto, K.; Watanabe, T. *Adv. Mater.* **1999**, *11*, 1365.
(15) Pastine, S. J.; Okawa, D.; Kessler, B.; Rolandi, M.; Llorente, M.; Zettl, A.; Frechet, J. M. J. *J. Am. Chem. Soc.* **2008**, *130*, 4238.
(16) Artus, G. R. J.; Jung, S.; Zimmermann, J.; Gautschi, H.; Marquardt, K.; Seeger, S. *Adv. Mater.* **2006**, *18*, 2758.
(17) Hosono, E.; Fujihara, S.; Honma, I.; Zhou, H. *J. Am. Chem. Soc.* **2005**, *127*, 13458.
(18) Feng, X.; Feng, L.; Jin, M.; Zhai, J.; Jiang, L.; Zhu, D. *J. Am. Chem. Soc.* **2004**, *126*, 62.
(19) Choi, J. H.; Kim, Y. M.; Park, Y. W.; Park, T. H.; Dong, K. Y.; Ju, B. K. *Nanotechnology* **2009**, *20*, 135303.

morphology and have no interactions between the adjacent sites. Nanoimprint techniques, with poly(dimethylsiloxane) (PDMS, Sylgard 184, Dow corning) flexible molds, are useful for the surface-texturing of polymer films because the polymer structures can be simply fabricated from a replica mold; this is economical and protects the quartz master from contamination during the fabrication process.[20,21]

Experimental Section

Fabrication of the Thin Gas Barrier. The thin gas barrier layers were coated on poly ethersulfone substrate (PES, 200 μm thickness). The Al_2O_3 barrier layer (~300 nm thickness) was deposited on both sides of a PES substrate by using an E-beam evaporator, and then the UV-curable polymer resin layer (about 1 μm thickness, Multicure 984-LVF, DYMAX Co.) was top-coated by dropping (on a 130 °C hot plate) on an Al_2O_3 layer.

Fabrication of a Flexible Mold from the Nanopatternd Quartz Master. A flexible PDMS mold has been fabricated by the solidification process on the nanostructured quartz master templates. The nanopattern on the quartz master was fabricated by laser interference lithography (LIL) process, based on the Lloyd's mirror interferometer using a 325 nm He−Cd laser.[22,23] A double-exposure and development process formed the dot patterns with ~400 nm diameter and ~700 nm center to center distance on the resist, and after the etching process, the dot pattern was transferred to the surface of the quartz master. Figure 1 shows the fabrication procedure of a PDMS, which is used for the nanoscale patterning material with high transmittance as a releasing mold. PDMS has a fairly low surface energy and provides easy release from the patterned polymer on the substrate.

Replication of Hydrophobic Surfaces with Nanoscale Resolution. Hydrophobic nanostructures on a flexible gas barrier substrate were fabricated by using a PDMS mold with ordered nanodot arrays that are inversely replicated from a quartz master template. An inversely patterned PDMS mold was pressed onto a UV-curable resin coated film, and the film was exposed to UV light (120 mW/cm^2 at 365 nm, CURE ZONE HO2, Daeho Glue Tech., Korea). After UV exposure for 2 min followed by baking at 130 °C for 60 min, the PDMS mold was peeled off. Because this UV-cured resin replica surface contains the nanodots and is inversely replicated from the PDMS mold with very low surface energy, this replica surface on a flexible PES film exhibits good hydrophobic properties. UV-cured resin is commonly used as a flexible gas barrier. We had performed the nanoimprint process on UV-curable resin, and it is a simple, fast, and low-temperature process.[19]

Deposition of SiO_2 Hydrophilic Dots. A structure mimicking the surface of the Stenocara beetle's back has been built by depositing an array of hydrophilic spots with size of ~500 μm onto a hydrophobic surface as shown in Figure 1. The optimum hydrophilic pixel size/center-to-center distance of 500 μm/1000 μm compares favorably with the hydrophilic/hydrophobic patterned back of the Stenocara beetle.[6] Finally, the hydrophilic regions were formed on the nanopatterned UV-cured resin layer by mesh-patterned mask deposition of SiO_2 inorganic material (~450 nm thickness and ~500 μm diameter).

Movement Mechanism of Moisture. The movement mechanism of moisture can be explained by the attractive force at interfaces. Fowkes,[24] in theoretical consideration of the attractive forces at the interface, has suggested that total free energy at a surface is the sum of contributions from the different intermolecular forces at the surface. Thus, the surface free energy of materials is the sum of hydrogen bonding and dispersion force components. Owens[25] calculated the surface energy (SE) from the contact angle measurements (CA) of water and formamide materials based on Fowkes' work. The SE is an important property of materials, generally characterized by measuring the CA of a liquid droplet sitting on the surface. We have measured the CA (Phoenix 450, Surface Electro Optic Co. Ltd., Korea) more than 10 times in each sample because CA measurement is highly sensitive to sample and environmental conditions.

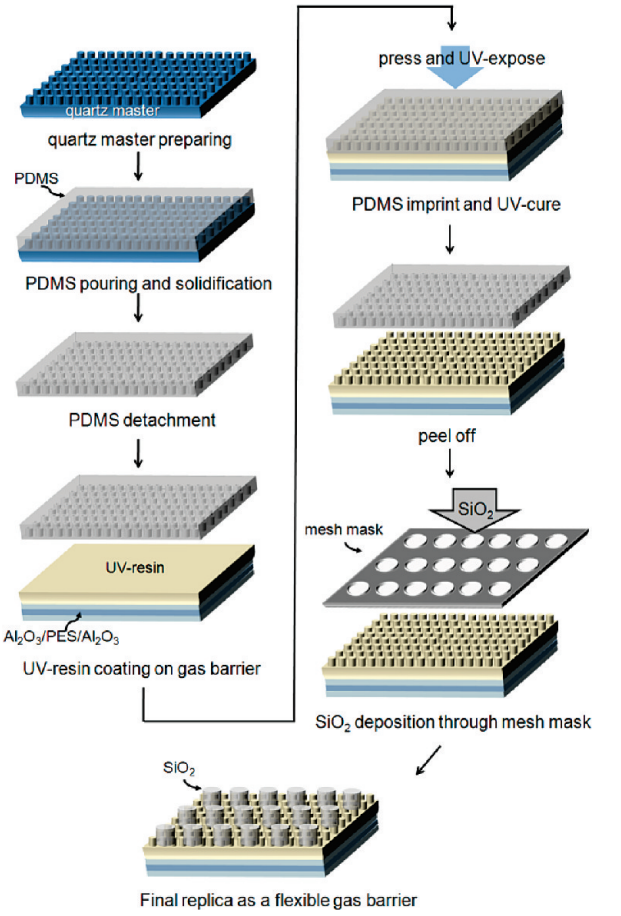

Figure 1. Schematic illustrations of inversely patterned PDMS solidification process on a nanopatterned quartz master, UV-imprinting procedure for the direct fabrication of a nanopatterned UV-cured resin as a hydrophobic surface by using a PDMS mold, and forming hydrophilic dot pattern as a final replica by mesh mask deposition.

Figure 2 shows the dynamic flow images of water droplets on plastic film divided by hydrophobic and hydrophilic regions. Water (20 μL) dropped on the hydrophobic region immediately moved to a hydrophilic area because of the difference of the SE. The water condensation image on the SiO_2 hydrophilic dots on the hydrophobic nanopatterned surface is shown in Figure 3a. In a humid condition, the droplets grow until they cover the entire hydrophilic bump, and then, under their own weight, they detach and roll downward. In this experiment, the humidity could affect moisture-controlling characteristics. Therefore, we have measured moisture permeation rates at 60 and 95% relative humidities (RH), respectively.

Structure of the Hydrophilic/Hydrophobic Surfaces. The dimensional qualities of the deposited SiO_2 hydrophilic regions and the nanopatterned UV-cured resin surface have been

(20) Kim, M.; Kim, K.; Lee, N. Y.; Shin, K.; Kim, Y. S. *Chem. Commun.* 2007, 2237.
(21) Kim, Y. S.; Suh, K. Y.; Lee, H. H. *Appl. Phys. Lett.* **2001**, *79*, 2285.
(22) Murillo, R.; van Wolferen, H. A.; Abelmann, L.; Lodder, J. C. *Microelect. Eng.* **2005**, *78*, 260.
(23) Cho, C.; Jeong, J.; Lee, J.; Jeon, H.; Kim, I.; Jang, D. H.; Park, Y. S.; Woo, J. C. *Appl. Phys. Lett.* **2005**, *87*, 161102.
(24) Fowkes, F. M. *Ind. Eng. Chem.* **1964**, *56*, 40.
(25) Owens, D. K.; Wendt, R. C. *J. Appl. Polym. Sci.* **1969**, *13*, 1741.

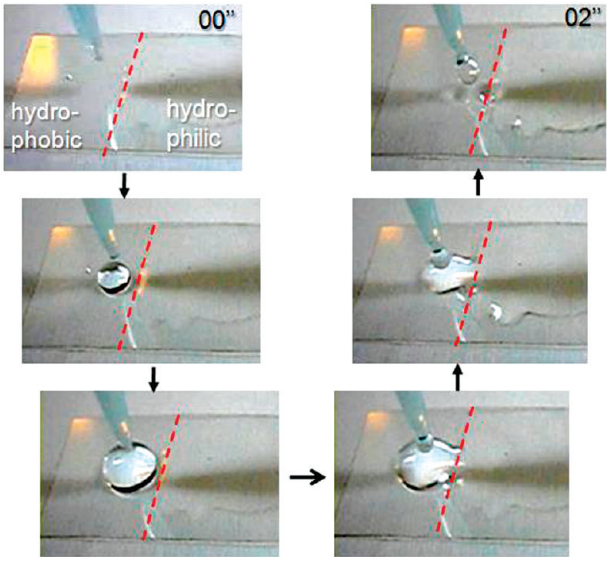

Figure 2. Dynamic flow images of water droplet (20 μL) on plastic film divided by hydrophobic and SiO_2 hydrophilic region in process of time.

characterized by a field-emission scanning electron micrograph (FE-SEM) and an atomic force microscope (AFM). Figure 3b shows FE-SEM images of the SiO_2 hydrophilic dot pattern (~500 μm in diameter) on a hydrophobic nanopatterned UV-cured resin surface, and Figure 3c shows magnified images of nanopatterned (~400 nm in width, ~200 nm in depth, and ~700 nm center to center) UV-resin replica fabricated by the imprinting techniques.[19] We have changed the surface roughness for the fabrication of the hydrophobic surface. The root-mean-square roughness of the flat UV-cured resin surface was 3.58 nm. The pattern uniformity of the surface is a major factor for use in a gas barrier. The ~400/~700 nm pattern showed better uniformity of the quartz master when it was fabricated by the LIL process.

Results and Discussion

Level of Surface Modification. Surface roughness is a main factor governing surface wettability. The level of modification of the surface was characterized by the static CA measurements. Deionized (DI) water droplet (20 μL) and formamide liquid (20 μL) were deposited on the sample surface using a micropipet, and a photograph of the water droplet was taken immediately with the goniometric camera. We have measured the CA on the flat SiO_2 surface (without patterning process) and on the nanopatterned hydrophobic surface (before SiO_2 deposition) on the film. The CA values were given by the software measurements, and the DI water and formamide CAs of the nanopatterned hydrophobic surface on barrier films had been measured to be 122 ± 1.5° and 110.2 ± 1.4°, respectively (7.29 mN/m of the SE) compared to the flat UV-cured resin surface, which gives values of 79.8 ± 1.3° and 72.8 ± 1.1°, respectively (25.8 mN/m of the SE).[19] Advancing (from 0 to 20 μL) and receding (from 20 to 0 μL) CAs on the nanopatterned hydrophobic surfaces were 131 ± 4.3° and 110 ± 5.4°, respectively. The wetting angle hysteresis was about 21°. The SE of the flat SiO_2 hydrophilic region (both CAs were < 5°) was > 73.12 mN/m calculated by Owen's equation and that was higher than surface tension of ordinary water substance (72.8 ± 0.7 mN/m).[24,25]

Therefore, a water vapor incident upon the hydrophobic regions is moved along the surface until it reaches a hydrophilic region because of the difference of the SE, the value of which was > 65.83 mN/m. Photographs of the film are shown in Figure 4a (DI water contact images of the flat UV-cured resin surface, nanopatterned hydrophobic surface (including advancing and receding contact angle images), and flat SiO_2 hydrophilic surfaces) and in Figure 4b (pattern-viewed tilted images that illustrate an array of circular hydrophilic spots with diameter of ~500 μm).

Moisture Permeation Rates. Moisture barrier properties have been characterized by measurements of the water vapor transmission rates (WVTR, g/m^2/day). A Ca test (refer to Supporting Information) using an electrical measurement of Ca degradation has been previously reported.[26] The schematic diagram of the Ca test is shown in Figure 5. The amount of oxidative degradation in a thin Ca sensor is monitored by resistance measurements. The water vapor, permeating through the gas barrier on PES, oxidizes the Ca. This is reflected by the decreasing current when a constant voltage is applied and monitored on a two-point probe system. Figure 6a shows the changes in the electrical transmission through the thin Ca in proportion to moisture permeation.

At 20 °C and 60% RH, the permeation curves of the hydrophilic/hydrophobic surface as a final replica sample, hydrophobic nanopatterned surface, and flat resin surface as a reference on the flexible gas barriers are presented in Figure 6a. The Al_2O_3 barrier layer, coated on both sides of PES film with flat resin, top coated on the Al_2O_3 layer, decreased the water permeation rates, which has a value of 9.8×10^{-3} g/m^2/day compared to 34.1 g/m^2/day for bare PES.

To demonstrate the behavior of moisture-repellent characteristics, the hydrophobic nanopatterned UV-cured resin surface on the barrier film (before SiO_2 hydrophilic dot deposition) has been measured under the same condition. The hydrophobic surface showed a better barrier performance with a permeability of 2.08×10^{-3} g/m^2/day compared to the flat resin surface. The permeation rates of the final replica produced by mimicking the surface of the beetle's back have been measured for verification of moisture transfer characteristics from hydrophobic domains to hydrophilic spots. The results indicate that this film gives more enhanced barrier performance. A permeability value of 5.34×10^{-4} g/m^2/day has been measured in relation to the time dependence function. These results show that the structure, which can control moisture, could effectively protect the film from moisture permeation. The major limitation of the test sensitivity is the film encapsulation. To test the amount of water permeation through the gas barrier, the device has been prepared on a glass substrate encapsulated by a glass lid, which led to a stable baseline value of $< 10^{-5}$ g/m^2/day.

The effectiveness of the surface modification depended on RH conditions.[27,28] As shown in Figure 6b, the concept of the surface modification for enhancement of gas barrier properties was more effective in the humid condition. At 20 °C and 95% RH, moisture permeation rates of the flat UV-cured resin surface, the hydrophobic surface, and the hydrophilic dots on the hydrophobic surface of a gas barrier film were 2.73×10^{-1}, 9.9×10^{-3}, and 2.01×10^{-3} g/m^2/day, respectively. The flat resin surface showed worse barrier characteristics in the humid condition. However, the hydrophilic/hydrophobic patterned surface and pure hydrophobic surface offered more powerful

(26) Choi, J. H.; Kim, Y. M.; Park, Y. W.; Huh, J. W.; Kim, I. S.; Hwang, H. N.; Ju, B. K. *Rev. Sci. Instrum.* **2007**, *78*, 064701.
(27) Jeyaprakash, J. D.; Samuel, S.; Ruther, P.; Frerichs, H.-P.; Lehmann, M.; Paul, O.; Ruhe, J. *Sens. Actuator B* **2005**, *110*, 218.
(28) liu, T.; Yin, Y.; Chen, S.; Chang, X.; Cheng, S. *Electrochim. Acta* **2007**, *52*, 3709.

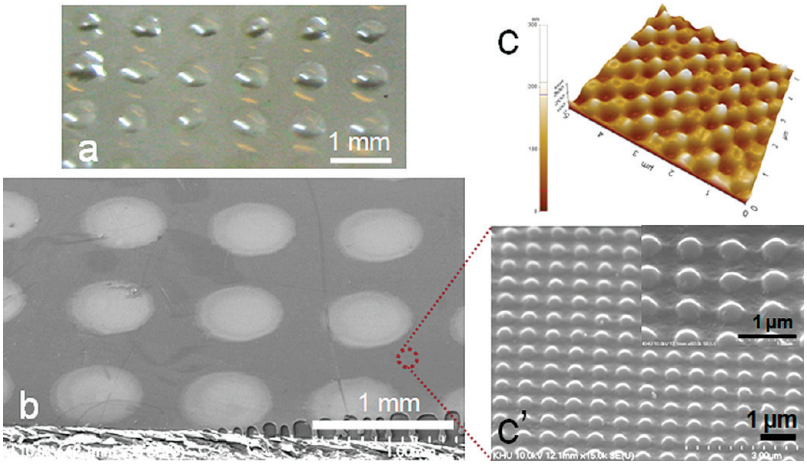

Figure 3. (a) Water condensation image on SiO_2 hydrophilic dots on hydrophobic nanopatterned surface, and FE-SEM images of (b) the SiO_2 hydrophilic dot pattern (~500 μm for a diameter) on a hydrophobic nanopatterned UV-cured resin surface and (c) a magnified AFM and SEM images of an imprinted hydrophobic surface (~400 nm in width, ~200 nm in depth, and ~700 nm center to center).

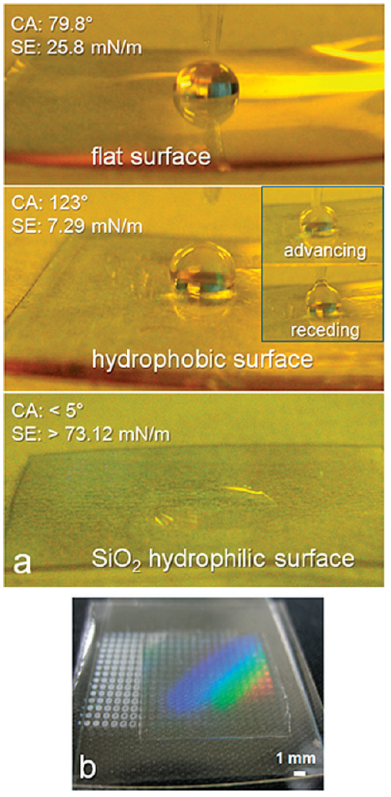

Figure 4. (a) DI water contact images of flat surface, nanopatterned hydrophobic surface and flat SiO_2 hydrophilic surfaces (including advancing and receding contact images) and (b) pattern-viewed tilted images of hydrophilic patterns on hydrophobic surfaces as a final replica of a flexible gas barrier film.

barrier characteristics in 95% RH. As shown in Figure 6c, moisture transfer characteristics (hydrophilic/hydrophobic) were more effective than moisture-repellent properties (hydrophobic) in relation to barrier efficiency at 95% RH.

A certain quantity of moisture moved by the hydrophilic dots permeated the gas barrier. In the humid condition, according to the moisture condensation mechanism of the Stenocara beetle's back, the water vapor combined with the vapor already present on the hydrophilic region continued to expand until they reached critical droplet size, and then they detached from the surface and fell off. High contrast between the hydrophilic and hydrophobic regions, higher resolution patterning process (free from distortion, cracks), longtime measurements, and a highly hermetic encapsulation process could provide clearer exploration of the mechanism. For this reason, this work remains to be performed for reproducible and consistent results.

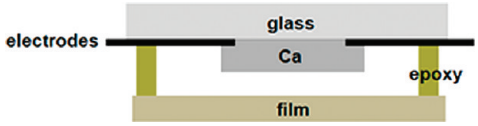

Figure 5. Schematic of the Ca test for the measurement of WVTRs.

Light Transmittance Values. With respect to the coating of film, the light transmittance is of major importance. The optical properties of the samples fabricated have been characterized by a UV−vis spectrometer, and the transmittances of the hydrophilic dots on the hydrophobic surface of the PES and reference films (air, bare PES, flat resin coated on PES, hydrophobic nanopatterned UV-cured resin surface) was measured. Figure 7 represents the transmittance spectrum in the visible region for the film after the SiO_2 deposition and PDMS imprinting process. The UV-curable resin has been found able to absorb the UV light in the range of about 220−420 nm. Compared with an 86% average transmittance value for bare PES, the average transmittances of the final replica, pure hydrophobic surface, and flat resin surface on gas barriers have been measured to be about 91, 92, and 87%, respectively. The transmittances obtained for the hydrophobic films, with and without SiO_2 dots, were higher than those of bare PES in the visible wavelength range. The blur of the surface roughness is mainly induced by Mie scattering effects,[29] which are dominantly effective on the structures that are comparable in size to the visible light wavelength. However, structures with nanosize dimensions on a film make the film more transparent. Introducing nanopattern into thin polymer films to reduce the effective refractive index of the polymeric material is a well-known technique for improving the performance of optical coating.[20] As can be seen in the inset of Figure 7, the name card underneath the final replica is not blurred, and the RGB colors were clearly visible. This result showed that the

(29) Mie, G. *Ann. Phys.* **1908**, *25*, 377.

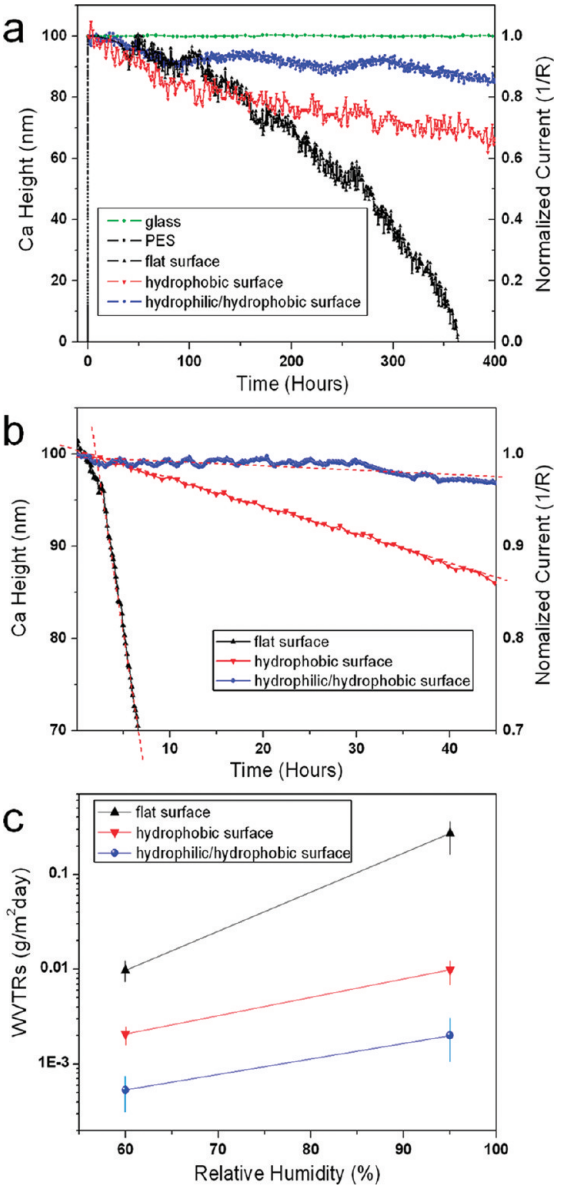

Figure 6. (a) Permeation curves of the flat UV-cured resin/Al_2O_3/PES/Al_2O_3, nanopatterned UV-cured resin/Al_2O_3/PES/Al_2O_3, and SiO_2 dots/nanopatterned UV-cured resin/Al_2O_3/PES/Al_2O_3. The slopes of the linear fit of the films yield the WVTRs 9.8×10^{-3}, 2.08×10^{-3}, and 5.34×10^{-4} g/m^2/day at 20 °C and 60% RH, respectively. The pure glass and bare PES were used as references. (b) Permeation curves of the films at 20 °C and 95% RH. (c) Permeation rates of the films at 60 and 95% RH (at 20 °C).

formation of uniform and constant nanopatterns can be applicable to optic devices.

Conclusion

Hydrophilic patterns have been fabricated on a hydrophobic surface with moisture-controlling characteristics similar to the surface of the Namib Desert beetle's back. In this work, we have demonstrated moisture barrier properties by controlling the movements of moisture. Water vapor incident upon the nanopatterned hydrophobic UV-cured resin region was efficiently moved along the surface until it reached a SiO_2 hydrophilic region (500/1000 μm, diameter/center to center). This concept can be effective for the design of gas barrier films and lead to enhanced barrier performances. The proposed approaches are suitable for various applications that require hydrophobic, low temperatures, and transparent surface coating technologies. This strategy can be easily extended to large area patterning; therefore, this simple and fast method could be ideally suitable to developing mass production solutions for nanopatterned polymeric optical substrates, which are adaptable to such cases as organic electronics, solar cells, and plastic optics applications requiring moisture-free properties with high transmission.

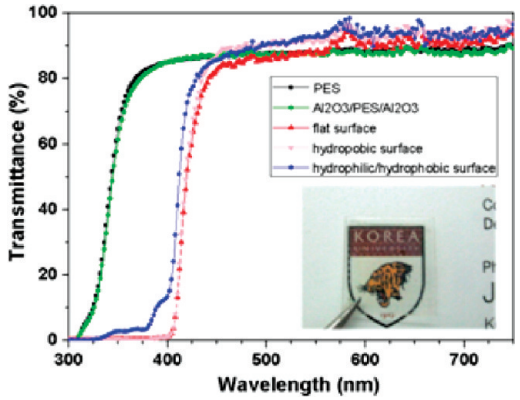

Figure 7. Transmittance graph of the final replica as a flexible gas barrier with reference films and a photograph of the name card underneath the film.

Acknowledgment. This work was supported by a Grant-in-Aid (10030041-2008-12) for Next-Generation New Technology Development Programs from the Ministry of Knowledge Economy of the Korean government and by the National Research Laboratory (R0A-2007-000-20111-0) Program of the Ministry of Education, Science and Technology (Korea Science and Engineering Foundation); this work was also supported by a Korea Science and Engineering Foundation (KOSEF) grant funded by the Korea Ministry of Education, Science and Technology (MEST) (No. R11-2007-045-01003-0). J.H.C. thanks the Seoul Metropolitan Government for the Seoul Fellowship.

Supporting Information Available: Derivation of moisture permeation rates using electrical measurements of Ca oxidation, with chemical equation, schematic diagram, and permeation curve of glass in detail, with measurements images. This material is available free of charge via the Internet at http://pubs.acs.org.